

NACA TN 3202

NATIONAL ADVISORY COMMITTEE FOR AERONAUTICS

TECHNICAL NOTE 3202

OSCILLATING PRESSURES NEAR A STATIC PUSHER PROPELLER AT
TIP MACH NUMBERS UP TO 1.20 WITH SPECIAL REFERENCE
TO THE EFFECTS OF THE PRESENCE OF THE WING

By Harvey H. Hubbard and Leslie W. Lassiter

Langley Aeronautical Laboratory
Langley Field, Va.



Washington

July 1954

ERRATA

NACA TN 3202

OSCILLATING PRESSURES NEAR A STATIC PUSHER PROPELLER AT
TIP MACH NUMBERS UP TO 1.20 WITH SPECIAL REFERENCE
TO THE EFFECTS OF THE PRESENCE OF THE WING
By Harvey H. Hubbard and Leslie W. Lassiter

April 1954

Page 8, line 27: The factor 480 appearing in the denominator on the right of this equation should be in the numerator instead.

Page 31: In the title of figure 15, the quantity $x/r = 0.50$ should be $x/r = 0.25$.

TECHNICAL NOTE 3202

OSCILLATING PRESSURES NEAR A STATIC PUSHER PROPELLER AT
TIP MACH NUMBERS UP TO 1.20 WITH SPECIAL REFERENCE
TO THE EFFECTS OF THE PRESENCE OF THE WING

By Harvey H. Hubbard and Leslie W. Lassiter

SUMMARY

Measurements of free-space oscillating pressures near a static propeller in the region where a wing might be located are presented for the tip Mach number range of 0.50 to 1.20 and these results are compared with available theory. Some measurements are also presented which were made near the tips in the region where a fuselage might be located in order to extend the range of existing data from a tip Mach number of 1.00 to 1.20. In addition to a description of the free-space pressure field, measurements are given for some of the same field points with a wing in place.

The radial pressure distributions vary as a function of axial distance and order of the harmonic. The maximum pressures occur at a greater radial distance as the axial distance is increased and as the order of the harmonic increases. The pressures generated per unit power for the lower harmonics tend to decrease and for the higher harmonics tend to increase with an increase in tip Mach number. In the region outboard of the propeller tips, some of the higher harmonics have a greater amplitude than the lower ones at supersonic tip speeds; whereas, in the region inboard of the propeller tips, the lower harmonics have the greatest amplitudes at all tip Mach numbers up to 1.20.

The direction of rotation is significant with regard to the magnitudes of wing surface pressures. Pressure magnitudes higher than free-space values are measured on surfaces which the blade approaches; whereas values lower than free-space values are measured on the surface from which the blade recedes. Differential pressures measured across a thin wing are greater than the free-space values at corresponding field points.

The theory of NACA Report 996 was found useful for calculations inboard of the propeller tips and for tip Mach numbers up to 1.20. When all steady forces are assumed to be concentrated at a single effective radius, the maximum pressure amplitudes can be calculated fairly well but the radial pressure distributions are somewhat distorted. If more detailed information concerning the distribution of these pressures is desired, a more cumbersome method of calculation which has given excellent results by use of torque and thrust forces distributed along the blade may be used.

INTRODUCTION

A rotating propeller is an intense source of oscillating pressures. At large distances from the propeller, these pressures are recognized only as noise, whereas at points in the immediate vicinity of the propeller they are of such magnitude that they are also capable of exciting destructive vibrations in nearby parts of the airplane structure. Such vibrations are excited at the blade-passage frequency of the propeller or at some integral multiple of that frequency. The fatigue problem associated with vibrations of this nature is a serious one since, with excitation frequencies of the order of 100 cycles per second, the structure may be subjected to a varying stress several millions of times during a single flight. The fatigue of metal parts is thus greatly accelerated and several instances of resulting failures of the secondary structure of wings and fuselages have been reported. The proposed use of propellers with higher tip speeds and of more powerful engines will intensify this already serious problem.

The work of reference 1 considers the fuselage-wall vibration problem and describes the oscillating-pressure field in the region where a fuselage might be located. A theory is given for calculating the free-space oscillating pressures associated with a rotating propeller at any point in space, and satisfactory experimental verifications are given for the region outboard of the propeller tips in the tip Mach number range up to 1.00. There were no attempts in the work of reference 1 to make measurements or apply the theory in the region inboard of the propeller tips or for tip Mach numbers above 1.00.

The experimental work of the present report was aimed primarily at a survey of the oscillating-pressure field in the region of a wing for a pusher-propeller configuration at tip Mach numbers up to 1.20. Some data were also obtained for the purpose of extending the data of reference 1, for the region of the fuselage, to supersonic tip Mach numbers. Charts based on experimental data are presented to enable a designer to estimate the maximum free-space oscillating pressures near the propeller at tip Mach numbers up to 1.20. Measurements were made at the same field points both with and without a thin wing in place to evaluate the effects of the wing.

Experimental results have been compared with the theory of reference 1 for both subsonic and supersonic tip Mach numbers and at various field points both inboard and outboard of the propeller tips. Some calculations made by the assumption of an effective-radius concept, as in reference 1, are compared with a more exact calculation wherein a radial integration was performed.

SYMBOLS

b	blade width
B	number of blades
c	speed of sound
$C_P = P/\rho n^3 D^5$	
d	tip clearance
D	propeller diameter
h	maximum thickness of blade section
$k = mB\omega/c$	
m	order of harmonic
M_t	tip Mach number (rotation only)
n	propeller rotational speed
p	root-mean-square free-space oscillating pressure of a given harmonic
P_c	free-space oscillating pressure coefficient, $p/\rho n^2 D^2$
P_{max}	maximum root-mean-square free-space oscillating pressure
P_p	peak-to-peak oscillating pressure
P	power absorbed by propeller
P_O	disk power loading of propeller
Q	torque of propeller
r	station radius
R	propeller radius
R_e	effective propeller radius

S_e	distance from field point to doublets at effective propeller radius
T	thrust of propeller
x, y, z	Cartesian system of coordinates, propeller axis along x-axis
β	blade angle
θ	angle between y-axis and radius of doublet circle
ρ	density of air
$X = r/R$	
ω	angular velocity

EQUATION FOR FREE-SPACE PRESSURES

The equation used for calculating free-space pressures has been derived in reference 1. This equation, which gives the absolute value of the root-mean-square pressure for any given harmonic, is given for convenience as follows:

$$\begin{aligned}
 p = \frac{1}{4\pi^2 \sqrt{2}} & \left[\left\{ \int_0^{2\pi} \left(T_x + \frac{Qy \sin \theta}{R_e} \right) \frac{1}{S_e^3} \left[\cos(mB\theta + kS_e) + \right. \right. \right. \\
 & \left. \left. \left. kS_e \sin(mB\theta + kS_e) \right] d\theta \right\}^2 + \left\{ \int_0^{2\pi} \left(T_x + \frac{Qy \sin \theta}{R_e} \right) \frac{1}{S_e^3} \left[kS_e \cos(mB\theta + \right. \right. \right. \\
 & \left. \left. \left. kS_e) - \sin(mB\theta + kS_e) \right] d\theta \right\}^2 \right]^{1/2} \quad (1)
 \end{aligned}$$

where $S_e = \sqrt{x^2 + y^2 + R_e^2 - R_e y \cos \theta}$, the distance from the field point to the doublets of the effective propeller circle as indicated in figure 1. The quantities T and Q are the thrust and torque, respectively; m is the order of the harmonic; B is the number of blades; $k = mB\omega/c$, where ω is the angular velocity and c is the speed of sound; and x and y are coordinates of the field point $(x, y, 0)$. The parameter R_e

is defined as an effective propeller radius and the torque and thrust forces are assumed to be concentrated at that station on the blade. When thrust and torque are given in pounds and pound-feet, respectively, and the distances are in feet, the pressure is calculated in pounds per square foot.

APPARATUS AND METHODS

Most of the testing was done with a 3.92-foot-diameter propeller which incorporated NACA 4-(5)(08)-03 blades, shortened and made square at the tips. This is the same propeller as was used for the tests of reference 2, and a photograph of it and its drive system is shown in figure 2 of that report. The remainder of the testing was done with a 3.50-foot-diameter propeller which incorporated NACA 4-(3)(08)-03 blades that were shortened and made square at the tips. The blade-form curves for these two propellers are given in figure 2.

The test propellers were driven by 200-horsepower water-cooled variable-speed electric motors. In order to achieve some of the higher tip speeds of the tests, two of these motors were coupled in tandem. Power absorbed by the motors was measured by means of a wattmeter; motor-efficiency charts were used to determine power absorbed by the propellers.

Measurements were made at several known distances from the propeller in a plane parallel to the ground and containing the propeller axis of rotation. Data were obtained for essentially free-space conditions and also for the case where a simulated wing surface was inserted in the pressure field. In the latter case, wing surface pressures as well as the differential pressures across the wing due to the propeller were measured. The dashed lines of figure 3 indicate the stations at which pressure surveys were made in both the axial and radial directions.

The simulated wing for these tests was a 3/4-inch-thick piece of plywood, 4 feet wide and 8 feet long, set at zero angle of attack and reinforced in order to minimize the effects of mechanical vibrations on the pressure measurements. The wing-propeller combination was set up as a pusher configuration with the propeller plane of rotation located 1/4 radius behind the wing trailing edge. Only one pressure-gage location was used, that being midway of the wing span and 1/4 radius from the trailing edge. Provision was made to move the wing assembly in order that data for various field points could be obtained.

Oscillating pressures were detected by means of a commercial crystal-type microphone which was shock mounted. The sensitive element has a flat response in the frequency range of 20 to 20,000 cps and is approximately 5/8 inch in diameter. Distortion of the pressure field due to its

small size is considered negligible. Because of the height of the propeller above the ground and the close proximity of the field points to the propeller, the pressures measured are essentially free-space pressures unless otherwise noted.

NACA miniature electrical pressure gages for measuring oscillating pressure, as described in reference 3, were flush mounted in each surface of the simulated wing. The individual gage outputs were recorded for purposes of studying the surface pressures on the wing. In order to measure the differential pressures at a given field point, a single gage was embedded in the wing and was vented to the surfaces by means of tubes of equal length. The frequency response was flat to approximately 5,000 cps for the flush-mounted gage and to approximately 3,500 cps for the gage-tube configuration. For all wing data, use was made of a filter arrangement such that the frequency response of the entire system was flat to 2,500 cps.

The output signals of the microphone and pressure-gage system were fed into a cathode-ray oscillograph and a Panoramic Sonic Analyzer in order to obtain the wave forms and frequency analyses. Permanent records of these data were made by photographing the viewing screens of the oscillograph and analyzer.

RESULTS AND DISCUSSION

The tests of reference 1 have shown that the magnitudes and frequency spectrums of the oscillating pressures near the tips of rotating propellers are largely a function of the tip Mach number and power coefficient of the propeller and of the location of the field point. The present tests extend the tip Mach number range of those experiments to 1.20 and provide some data inboard of the propeller tips in the region where a wing might be located. Data for some field points were obtained both with and without a wing in place for comparison.

FREE-SPACE PRESSURES

Discussion of the free-space pressures is divided into three parts. Experimental results in the form of amplitudes and frequency spectrums at various positions in the pressure field are first discussed. These results are then compared with some calculations by the theory of reference 1. Finally, some charts based on experimental results are presented so that maximum free-space pressures can be estimated for regions typical of those in which a wing or fuselage may be located.

Experimental Results

Experimental data for these studies were recorded in two general forms as illustrated in figures 4 and 5. Conventional cathode-ray oscillograph pictures of the overall signal, such as are shown in figure 4, were used to determine the peak-to-peak values of pressure. A blip in the light trace corresponds to a propeller blade passage; hence, each photograph of figure 4 shows two blade passages. For a propeller operating at a given blade angle and for which the aerodynamic forces on the blades are steady with time, these wave forms recur at the same magnitude as a function of time. Although these waves are markedly nonsinusoidal, they may be broken down into Fourier components. All individual components of the overall signals have a constant amplitude; hence, it was particularly convenient to perform frequency analyses by the use of a panoramic type of analyzer. Viewing-screen presentations of this analyzer, as shown in figure 5, give the root-mean-square pressure amplitude in logarithmic units on the vertical scale as a function of frequency on the horizontal scale. From these records, the root-mean-square amplitudes of the various harmonics may be obtained directly.

Peak-to-peak pressures.- Measured values of peak-to-peak pressure in pounds per square foot, as obtained from records of the type shown in figure 4, are plotted in figure 6 as a function of radial distance at a given axial distance and for various propeller rotational tip Mach numbers. It may be seen that the magnitudes increase rapidly as the tip Mach number increases. Relatively small values were measured for the lower tip Mach numbers, the greatest increase occurring as the tip Mach number exceeded 0.90. It may also be noted that the largest values were measured at field points near the propeller tip ($y/R = 1$) and in some cases outboard of the tip. Past experience has shown that the oscillating pressures generated by a propeller are closely related to the steady forces on the blades. Thus, changes in the free-space pressure distributions as noted in figure 6 are probably associated in some way with changes in load distributions on the blades.

Harmonic analyses.- The pressure fields generated by propellers are known to be rich in harmonics. This high harmonic content is believed to result from the impulse type of force applied to the air by the blade (ref. 4). Pressure waves having large harmonic contents are markedly nonsinusoidal, such as those in figure 4 which apply to a specific propeller. These pressure waves were recorded at a location near the propeller tip in the plane of rotation at three different test conditions, in order to illustrate some of the various wave shapes encountered. Although differences in shape are evident, these waves are of the same general type in that the peaks persist for only a small part of the cycle. For waves of this type, the magnitude of the peak-to-peak value is indicative of the frequency content of the wave. Those with a high peak-to-peak value have a greater harmonic content than those with a lower peak-to-peak value.

A quantitative indication of this trend is given in table I where harmonic analyses are given for the three waves of figure 4 which have progressively larger peak-to-peak values. (In the interpretation of the pressure values of table I, it should be borne in mind that the peak-to-peak value of a sine wave p_p is approximately 2.8 times its root-mean-square value p .) It can be seen that all three of these waves have large harmonic contents; however, the largest harmonic content is associated with the wave which has the largest peak-to-peak value. It may be noted, for instance, that the harmonics of wave form (a) are relatively lower in amplitude than its fundamental, whereas several harmonics of wave form (c) are higher in amplitude than its fundamental. It is evident from the values in the table that the pressure amplitudes of the higher order harmonics increase at a much more rapid rate than those of the lower order as the peak-to-peak values increase. In the present tests, wave forms of the type shown in figure 4(c) were encountered mainly at high tip speeds and/or at field points close to the propeller tips.

Figure 5 gives a qualitative picture of the experimentally determined free-space pressures near a propeller at y/R values from 0.25 to 1.75 for three different tip Mach numbers. This figure is made up from photographs of the viewing screen of the Panoramic Frequency Analyzer showing directly the pressure amplitudes for various frequencies. Both the vertical and horizontal scales are logarithmic and the gain settings are identical for all records shown. Root-mean-square pressure amplitudes p , which for convenience were recorded on a decibel scale, can be converted, if desired, to units of pounds per square foot by means of the following relation:

$$\text{Decibels} = 20 \log_{10} \frac{p}{0.0002 \times 480}$$

All data at any given Mach number are directly comparable. If data for different Mach numbers are compared, it should be noted that the power loading of the propeller differs with tip Mach number as shown in the figure.

It is seen that for the inboard stations the pressure field is made up largely of the low-frequency components; whereas, at stations near the tip and beyond, the higher frequency components are relatively strong. This latter effect is especially noticeable at the higher tip speeds.

Some of the data of figure 5 have been plotted in figure 7 to indicate the nature of the radial pressure distribution for the first, third, and fifth harmonics of a two-blade propeller. Pressures in pounds per square foot are plotted as a function of radial distance for a propeller tip Mach number of 1.10. For the conditions of the figure it can be seen that inboard of the propeller tip the lower order harmonics have the

higher values. Outboard of the tip, the higher order harmonics have the higher values. There is thus a trend such that the maximum point of the radial pressure distribution occurs at a point farther outboard for the higher order harmonics. This trend accounts for the widely different spectrums recorded in figure 5.

It was found during the course of the tests that the radial pressure distribution varied also as a function of the axial distance of the measurements. Data are shown in figure 8 for the fundamental frequency of a two-blade propeller at three different axial distances. Oscillating pressures in pounds per square foot are plotted as a function of radial distance for axial distances x/R of 0.25, 0.50, and 0.75. It can be seen that there is a tendency for the point of maximum pressure to move outboard at greater axial distances. Comparison of data at various tip Mach numbers indicated that Mach number had only a small effect on the location of the maximum pressures.

It appears that the shape of the radial pressure distributions as noted in figures 7 and 8 for the first few harmonics may be related to the axial distance in terms of the corresponding wave length. As an illustration, the location of maximum pressure for the third harmonic at an axial distance $x/R = 0.25$ would come at about the same radial station as for the first harmonic at an axial distance $x/R = 0.75$.

Comparison of Theory and Experiment

The available theory (eq. (1)) has been checked with experiments in the work of reference 1 and was found to be adequate for prediction of the pressure field in the region outboard of the propeller tips for tip Mach numbers as high as 1.00, which was the upper limit of those tests. In the work of the present report, some calculations were made for the region inboard of the tips as well as the outboard region and these results are compared with experiment for tip Mach numbers of 0.90 and 1.20. Most of the calculations were made by the use of an effective-radius concept, as in the work of reference 1, to simplify the numerical work. In addition, one example is given where a distribution of forces on the blades is assumed and a subsequent radial integration is performed in calculating the pressures.

Radial distance.— Figures 9 and 10 show the calculated root-mean-square pressure as a function of radial distance for the fundamental frequency of a two-blade propeller along with measured values, for Mach numbers of 0.90 and 1.20, and for x/R values of 0.25 and 0.50. For each of these conditions, calculations were made for effective-radius values of both 0.5 and 0.8. These values were chosen because in most cases the maximum measured values for the fundamental frequency were at radial stations between 50 percent and 80 percent of the tip radius. The theory

tends to predict a maximum in the pressure-distribution curve at the radial station at which the steady aerodynamic forces are assumed to be concentrated. The shapes of the calculated curves in all cases are somewhat different from the measured curves. In most cases, however, the maximum calculated values, especially those for $Re = 0.8$, agree fairly well with the maximum measured values and this agreement is approximately the same for both a subsonic and a supersonic tip Mach number.

Since the results of figures 9 and 10 showed that the shapes of the calculated pressure distributions inboard of the tips did not agree well with experiment when the assumption was made, as in equation (1), that the steady aerodynamic forces on the blades are concentrated at a given effective radius, it was of interest to check these results against those obtained by a calculation procedure where the thrust and torque were distributed along the blade. Results of these calculations are shown in figure 11 and are compared with the measured values for the conditions of figure 9(a). Torque and thrust distributions assumed in making these calculations are also given in the figure. The numerical work was done in four steps by assuming proportionate torque and thrust forces acting at the 0.3-, 0.5-, 0.7-, and 0.9-radius stations. It can be seen that the calculated values in figure 11 agree well with the measurements inboard of the tips, the agreement being much better than for the results of figure 9(a). These results are an indication that the basic concepts of the theory of reference 1 are valid but, for calculations in the region inboard of the tips, caution should be exercised in its use. It appears that calculations of the type for which results are presented in figure 11 may not be justified in most cases unless detailed information is needed because the maximum values calculated by equation (1) are usually in good agreement with the measurements. This result is fortunate since the designer will usually be concerned mainly about the maximum values encountered.

Axial distance.- Figure 12 presents the maximum calculated pressures of the fundamental frequency as a function of axial distance. It can be seen that the calculations show a very rapid drop off in pressure as the axial distance is increased. This trend is substantiated by the measured maximum values at three distances as shown in the figure.

Some calculations were made to compare the oscillating-pressure magnitudes ahead of and behind the propeller and these results are presented in figure 13. It can be seen that the calculated values indicate the same order of pressure magnitude for corresponding positions ahead of and behind the propeller plane. The limited amount of unpublished experimental data available tends to indicate also that the pressures ahead of and behind the propeller plane are of the same order of magnitude.

Charts for Estimating Free-Space Pressures

Although the theory is useful for predicting free-space pressures at field points near the propeller, the method of calculation is cumbersome. In reference 1, experimental data are presented in chart form in order to provide the designer with a means of rapidly estimating pressure magnitudes. Thus, for a given propeller, the pressures can be estimated quickly if power coefficient, tip Mach number, and tip clearance are known. The experimental results of the present tests are summarized in figures 14 and 15 from which more detailed charts of the type shown in figure 19 of reference 1 may be constructed.

Past experience has indicated that the fundamental blade-passage frequency is structurally of primary importance. It can be shown theoretically and has been confirmed experimentally that, for a given value of the product mB , the same pressure will be generated for different values of B . Thus, the data of figures 14 and 15, even though pertaining directly to a two-blade propeller, may be applied to propellers with a different number of blades.

Pressures in the region of the fuselage.- For a given tip clearance in the region of the fuselage, figure 21 of reference 1 gives the average values of pressure per unit power as a function of the propeller tip Mach number for various values of mB . The data of the present tests confirm the trends of reference 1 and allow an extension of the results to a tip Mach number of 1.20. Consequently, figure 14 has been prepared to include previously published data along with the more recent results in the region where a fuselage might be located. The maximum root-mean-square pressures generated per unit power for the lower harmonics tend to decrease and for the higher harmonics tend to increase with an increase in tip Mach number. These trends shown in the figure result in a "crossing over" of the curves in the vicinity of tip Mach number 1.00 in such a manner that the relative vertical position of the curves in the supersonic range is the reverse of that in the subsonic range. At subsonic speeds, the pressure per unit power is greater for the lower order frequencies; whereas, in the supersonic range, the pressure per unit power is relatively greater for the higher order frequencies.

Pressures in the region of the wing.- In order to provide charts for estimating pressures for the region near a propeller where a wing might be located, faired data have been plotted in figure 15 for an x/R value of 0.50. The data of figure 15 apply directly to a pusher-propeller configuration; however, there are indications, as in figure 13, that these results will apply approximately to tractor-propeller configurations also. These values represent the maximum values that would occur for any frequency and tip Mach number combination. These curves have the same general trends as the corresponding data of figure 14 except that the lower order frequencies have the highest pressure per unit power

throughout the entire tip Mach number range of the tests. Although the data of figure 15 are for a given value of x/R , the effect of distance, at least for the lower order harmonics, is indicated by figure 12. Thus, figures 12 and 15 may be used to estimate the maximum values of free-space pressure that will be encountered at any axial distance. The location of these maximum values, as shown elsewhere in the report, will probably occur at y/R values less than 1.0 except for some of the higher order frequencies.

WING PRESSURES

Previous discussion has dealt with the free-space oscillating-pressure field that exists in the region where a wing might be located. Some data were also recorded at the same field points with a thin wing in the pressure field and these are shown in figures 16 to 19. Surface pressures as well as the differential pressures across the wing were measured at various field points. These results apply directly to a relatively thin wing for a pusher configuration, and it is not known how the wing thickness affects the results.

Surface Pressures

Pressures were measured on both surfaces of the wing for various tip Mach numbers and at various field points. Both peak-to-peak values, obtained from wave forms of the type shown in figure 4, and root-mean-square values of various harmonics were determined for pressures which impinge on the wing panels.

Peak-to-peak values.- Figure 16 presents the peak positive and peak negative values of the pressures on two surfaces of a wing as a function of radial distance for various propeller tip Mach numbers. Peak-to-peak values can be obtained directly from figure 16 by addition of the positive and negative values on any given ordinate line. It will be noted that these values for either side of the wing are higher than corresponding free-space values shown in figure 6. It can also be seen that the negative values tend to be larger than the positive values for most of the cases shown and all pressures are greater on the surface approached by the blade than on the surface from which the blade recedes.

Harmonic analyses.- Ratios of the root-mean-square oscillating-pressure magnitudes at the surfaces of a thin wing to the corresponding free-space values for various harmonics of a two-blade propeller are given in figure 17. Since no apparent trend existed as a function of location of the field point or of propeller tip Mach number, the curves of figure 17 were obtained by averaging the values obtained at stations $y/R = 0.75, 1.00, \text{ and } 1.25$ for various tip Mach numbers. Compared with

the free-space values, the pressures on the surface from which the blade recedes are only slightly less. On the other hand, the pressures on the opposite surface which is approached by the blade are somewhat higher than the free-space values and the magnitudes vary as a function of the order of the harmonic, some of the higher harmonics being more noticeably affected.

Since large differences in the pressure magnitudes were detected for opposite sides of a wing, the direction of rotation appears to be a significant parameter. The large differences in pressure levels noted for opposite sides of the wing were also found to exist for the opposite direction of rotation except in the reverse sense. Thus, it appears that, in cases where the direction of rotation is fixed, some advantage can be taken of this difference in pressure magnitudes. Therefore, the critical surfaces will probably be on top of the wing on one side of the engine nacelle and on the bottom of the wing on the other side of the engine nacelle. These findings are consistent with those of reference 4 where it was shown theoretically that the direction of rotation is significant with regard to noise levels in airplane cabins when the wing blankets part of the pressure field.

Differential Pressures

The phase and magnitude differences between pulses impinging on the top and bottom surfaces of a wing cause an alternating differential pressure to exist across the wing. Near the trailing edge of the wing where the structure is relatively thin, this differential pressure may tend to flex the structure. For this reason, wing or aileron deformation may be most critical in the case of a pusher configuration such as the one for which these data were obtained.

Peak-to-peak values.- Figure 18 shows the peak-to-peak differential pressures across the wing as a function of radial distance for various tip Mach numbers. It can be seen that the pressure magnitudes increase as the tip Mach number increases in much the same manner as in free space. The magnitudes, however, are much greater than for the corresponding free-space points as indicated by a comparison of the curves of figures 6 and 18.

Harmonic analyses.- Figure 19 shows the root-mean-square differential-pressure amplitudes as a function of axial distance for various tip Mach numbers as compared with free-space measurements at the same field points. The differential pressures of fundamental rotational frequency are approximately 1.5 to 2.0 times the free-space values. Although complete data were not obtained, there is some evidence that the differential pressures of the higher harmonics may also be larger than the corresponding free-space values. In order to estimate the pressures tending to flex a wing, the data of figure 15 may be adjusted upward in accordance with the results of figure 19.

CONCLUSIONS

Studies of the oscillating pressure in the near field of a propeller operating at tip Mach numbers up to 1.20 for static conditions indicate the following conclusions:

1. Distributions of root-mean-square oscillating pressures measured along lines parallel to the propeller plane of rotation for a given axial distance vary widely as a function of tip Mach number and order of the harmonic. The maximum values of pressure occur inboard of the propeller tips for the fundamental frequency of a two-blade propeller; whereas, for the higher order harmonics, they occur near the propeller tip and in some cases outboard of the tip. The maximum measured values decrease rapidly and tend to move outboard as the axial distance is increased.

2. The maximum root-mean-square pressures generated per unit power for the lower harmonics tend to decrease and for the higher harmonics tend to increase with an increase in tip Mach number. In the region outboard of the propeller tips, some of the higher harmonics have a greater amplitude than the lower ones at supersonic tip speeds; whereas, in the region inboard of the propeller tips, the lower harmonics have the greatest amplitudes at all tip Mach numbers up to 1.20.

3. Peak-to-peak pressure magnitudes are greatest at radial stations near the propeller tips and increase rapidly as a function of tip Mach number.

4. The theory of NACA Report 996 for predicting the oscillating-pressure field of a propeller in the region outboard of the tips for tip Mach numbers up to 1.00 is also found adequate for calculations inboard of the propeller tips and for tip Mach numbers up to 1.20. Calculations for the inboard region were found to be rather sensitive to the assumed location of steady forces on the blades.

5. When the assumption is made that all steady forces are concentrated at a single effective radius, the maximum pressures can be estimated fairly well but the radial pressure distributions are somewhat distorted. If more detailed information concerning the distribution of these pressures is desired, a more cumbersome method of calculation which has given excellent results by use of torque and thrust forces distributed along the blade may be used.

6. Differential pressures measured across a thin wing are generally greater than the free-space values at corresponding field points.

7. The direction of rotation is significant with regard to the magnitudes of wing surface pressures. Pressure magnitudes higher than

free-space values are measured on surfaces which the blade approaches; whereas values lower than free-space values are measured on the surface from which the blade recedes.

Langley Aeronautical Laboratory,
National Advisory Committee for Aeronautics,
Langley Field, Va., April 15, 1954.

REFERENCES

1. Hubbard, Harvey H., and Regier, Arthur A.: Free-Space Oscillating Pressures Near the Tips of Rotating Propellers. NACA Rep. 996, 1950. (Supersedes NACA TN 1870.)
2. Hubbard, Harvey H., and Lassiter, Leslie W.: Sound From a Two-Blade Propeller at Supersonic Tip Speeds. NACA Rep. 1079, 1952. (Supersedes NACA RM L51C27.)
3. Patterson, John L.: A Miniature Electrical Pressure Gage Utilizing a Stretched Flat Diaphragm. NACA TN 2659, 1952.
4. Regier, Arthur A., and Hubbard, Harvey H.: Status of Research on Propeller Noise and Its Reduction. Jour. Acous. Soc. Am., vol. 25, no. 3, May 1953, pp. 395-404.

TABLE I
 ROOT-MEAN-SQUARE AMPLITUDES OF THE FIRST TWELVE ROTATIONAL
 HARMONICS OF THE WAVE FORMS OF FIGURE 4

Wave form (see fig. 4)	P_p , lb/sq ft	p, lb/sq ft, for -											
		m = 1	m = 2	m = 3	m = 4	m = 5	m = 6	m = 7	m = 8	m = 9	m = 10	m = 11	m = 12
(a)	9.8	1.6	1.0	0.8	0.7	0.6	0.4	0.4	0.3	0.2	0.2	0.1	0.1
(b)	98	5.9	4.7	4.7	4.4	4.4	4.2	3.7	3.0	2.6	2.1	2.0	1.6
(c)	980	33.1	37.2	39.7	41.7	41.7	37.2	37.2	35.2	35.2	33.1	31.3	29.4

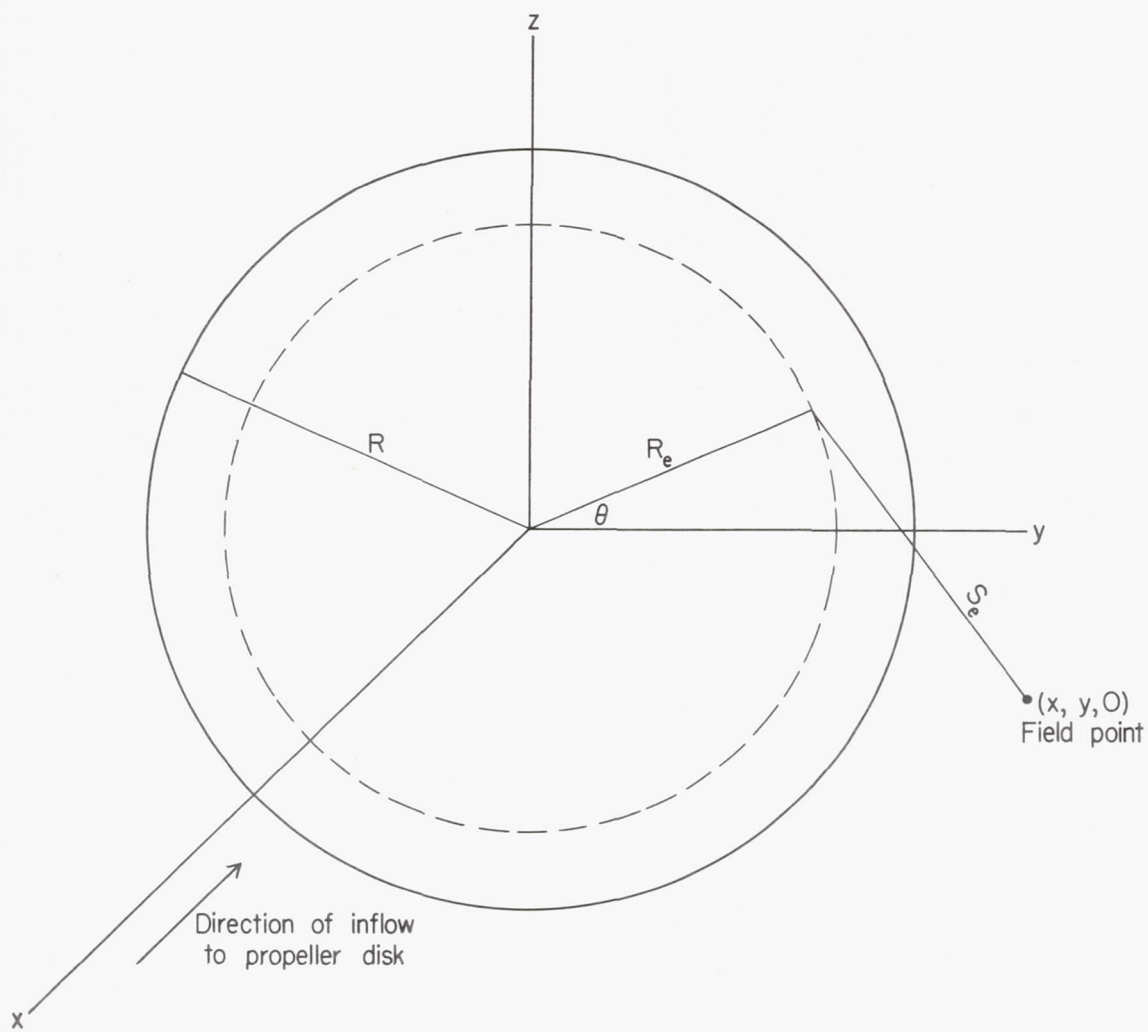


Figure 1.- Description of coordinate system.

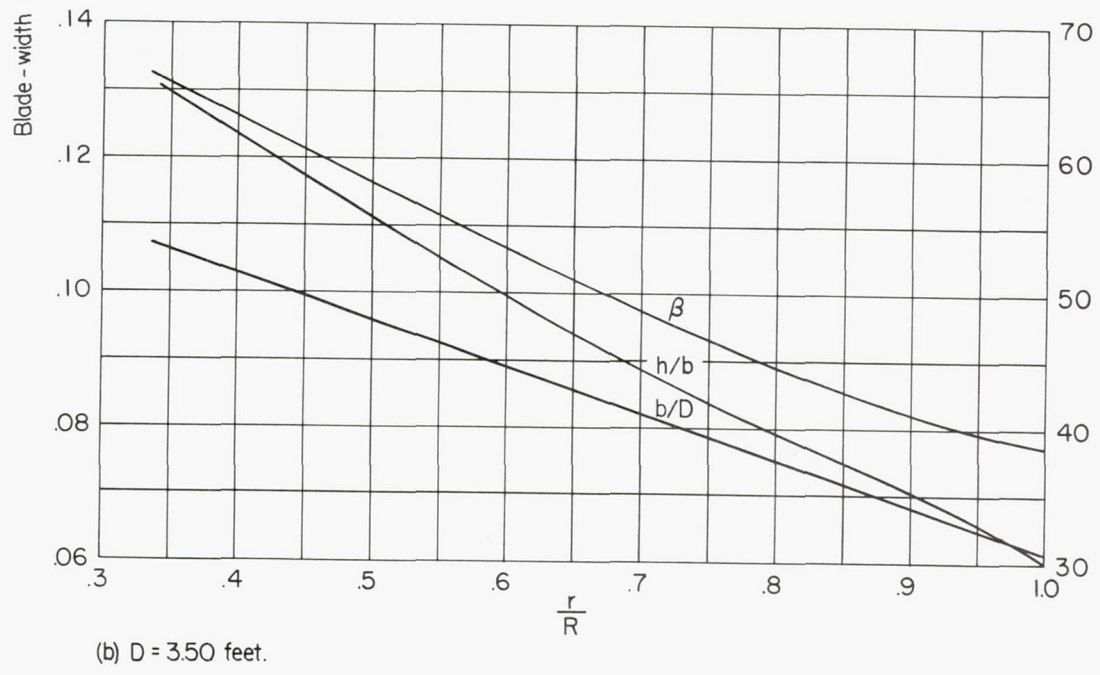
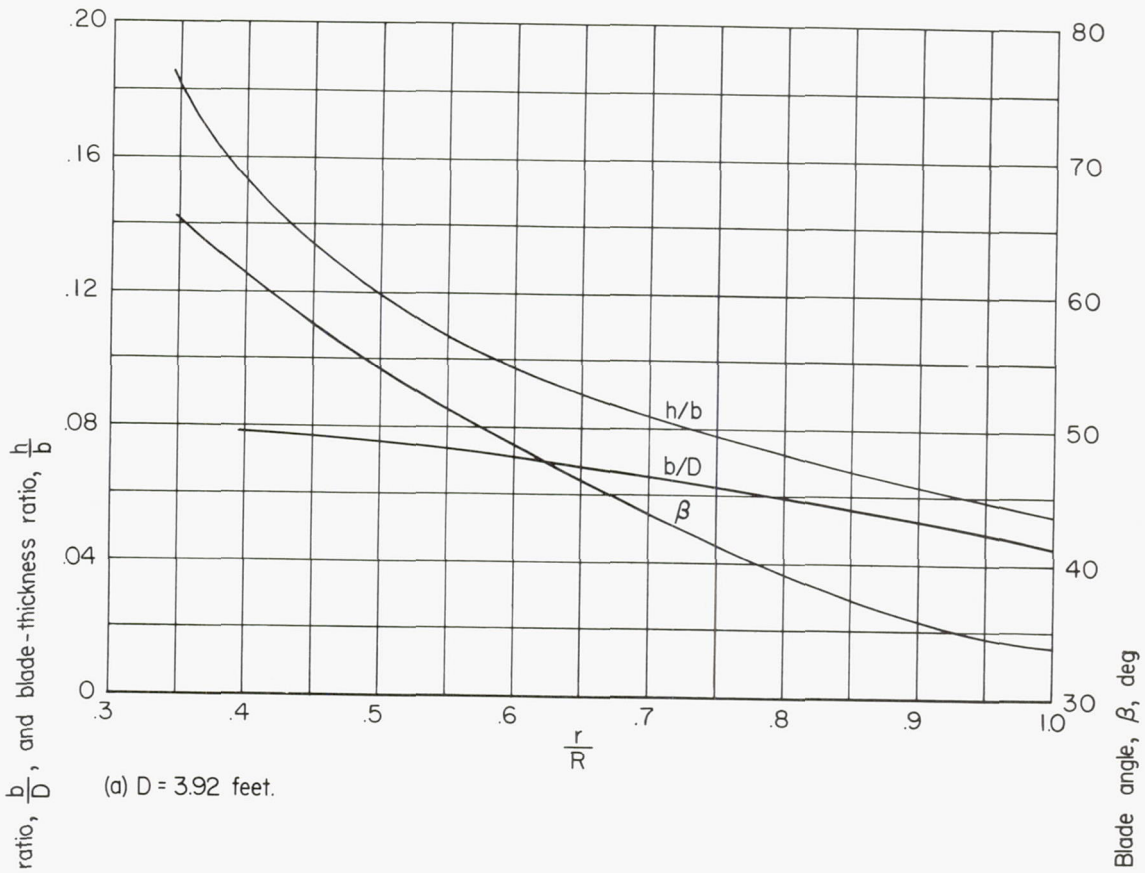


Figure 2.- Blade-form curves for test propellers.

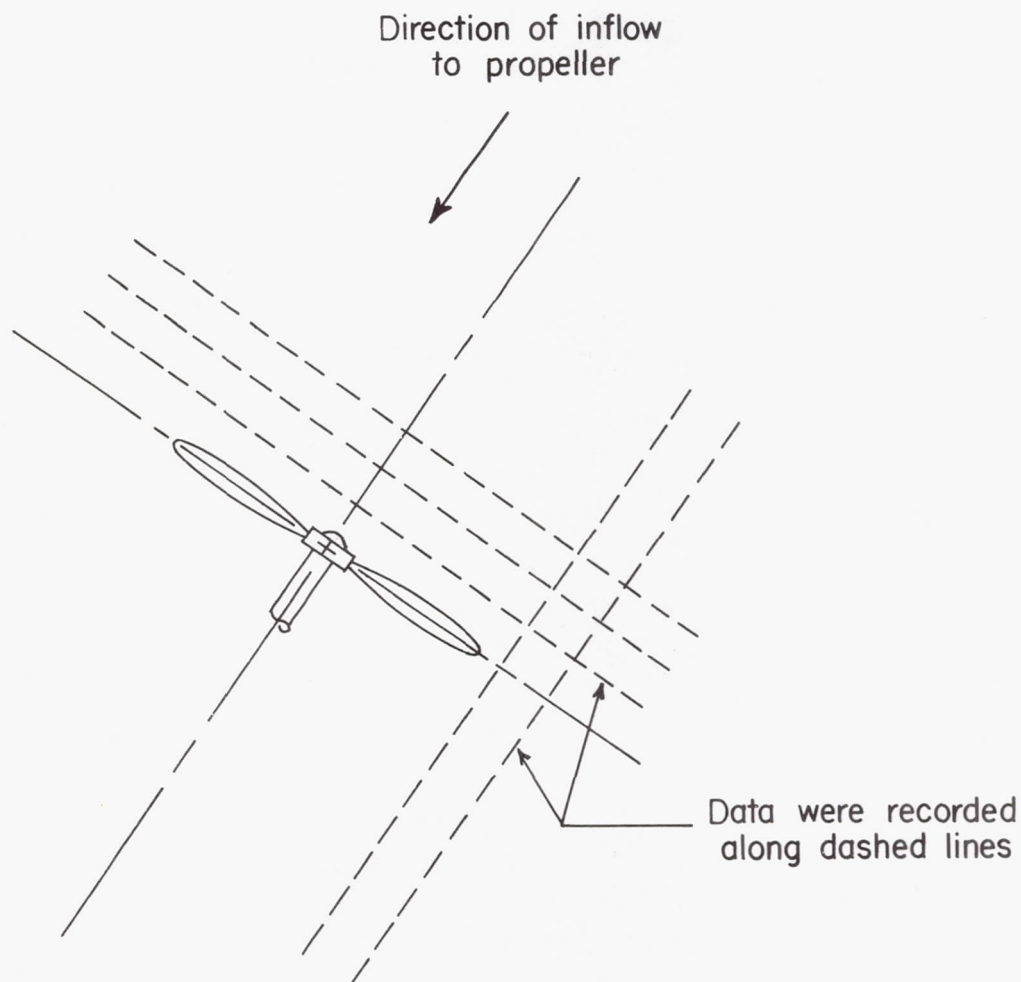
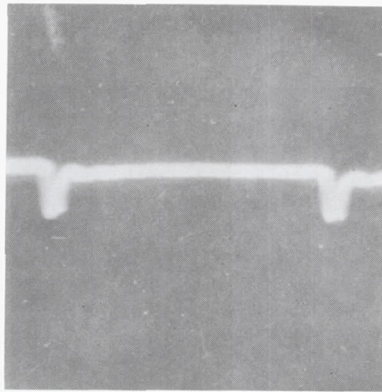
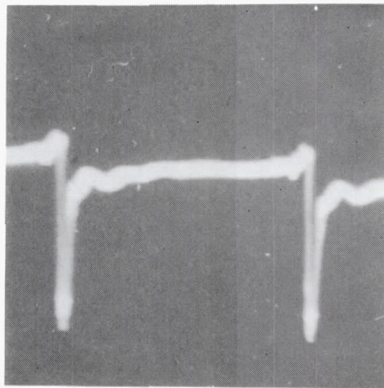


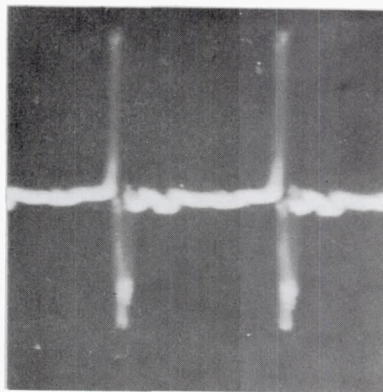
Figure 3.- Lines along which free-space and wing pressure surveys were made in a plane parallel to the ground and containing the propeller axis of rotation.



(a) $p_p = 9.8$ lb/sq ft.



(b) $p_p = 98$ lb/sq ft.



(c) $p_p = 980$ lb/sq ft.

Figure 4.- Sample pressure wave forms. (The root-mean-square pressure amplitudes of some of the harmonics are given in table I.)

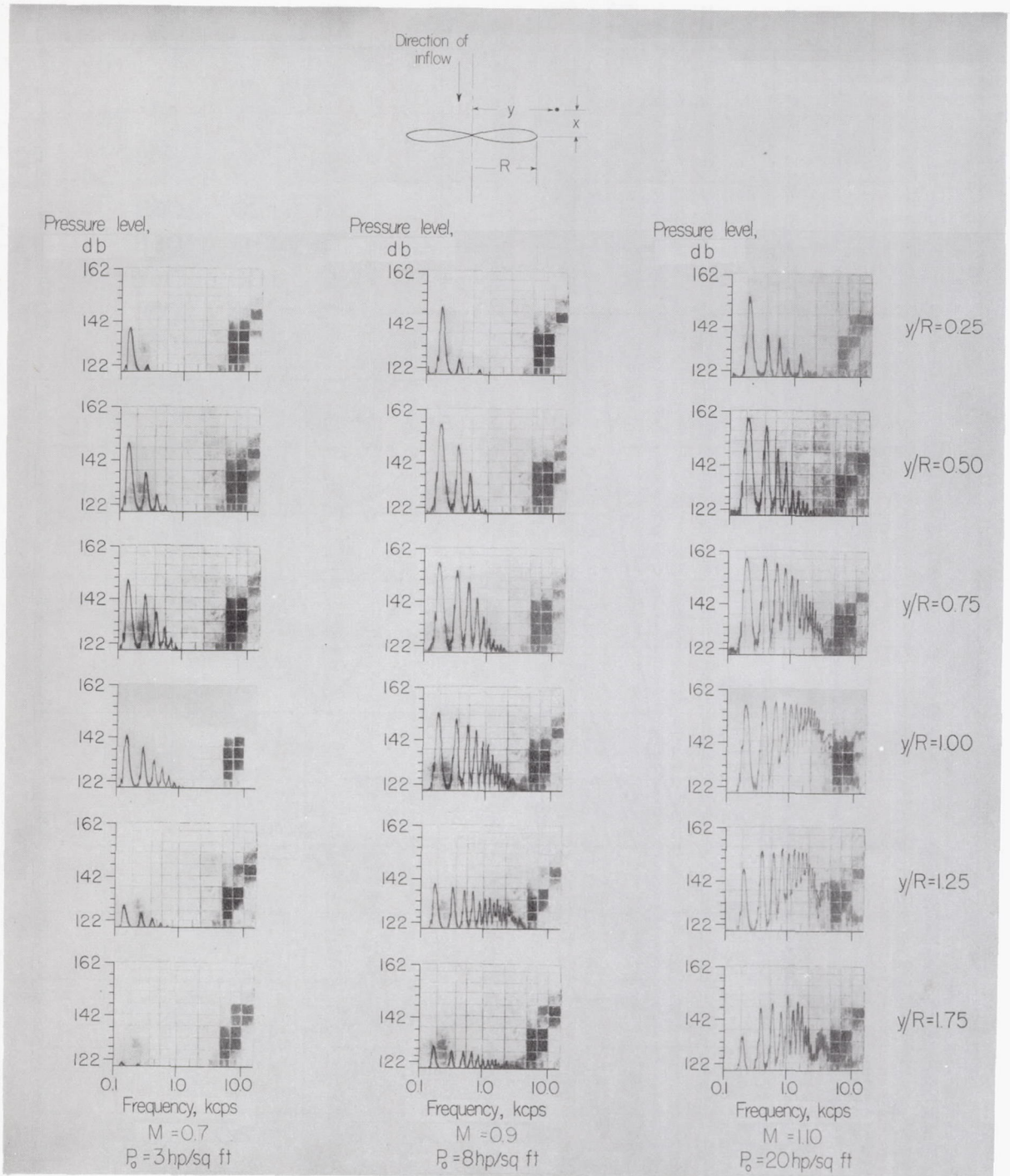


Figure 5.- Spectrums showing variation of frequency content as a function of radial distance from the propeller axis for three tip Mach numbers. $x/R = 0.25$.

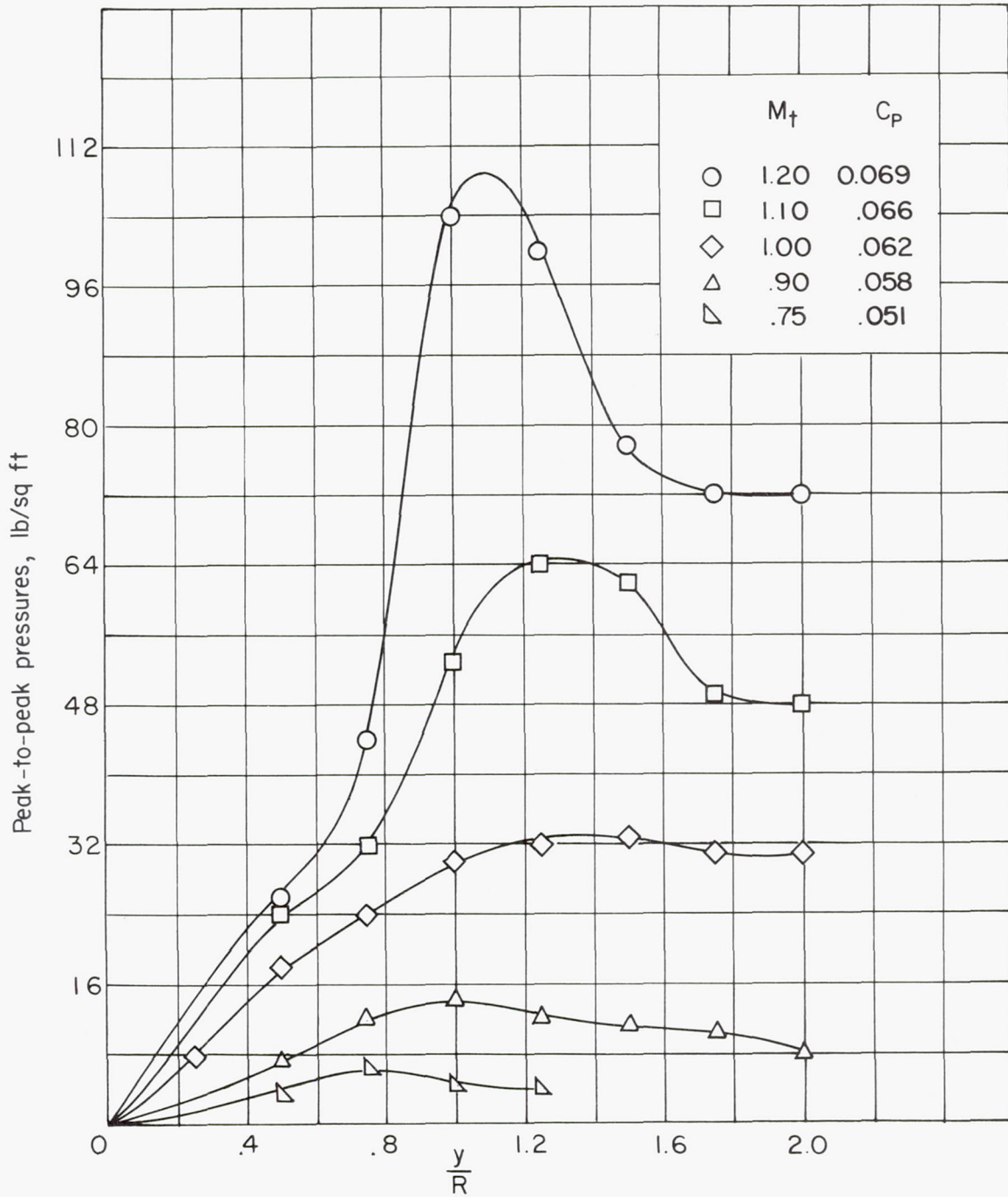


Figure 6.- Free-space peak-to-peak pressures for a two-blade propeller as a function of radial distance for various tip Mach numbers. $x/R = 0.50$.

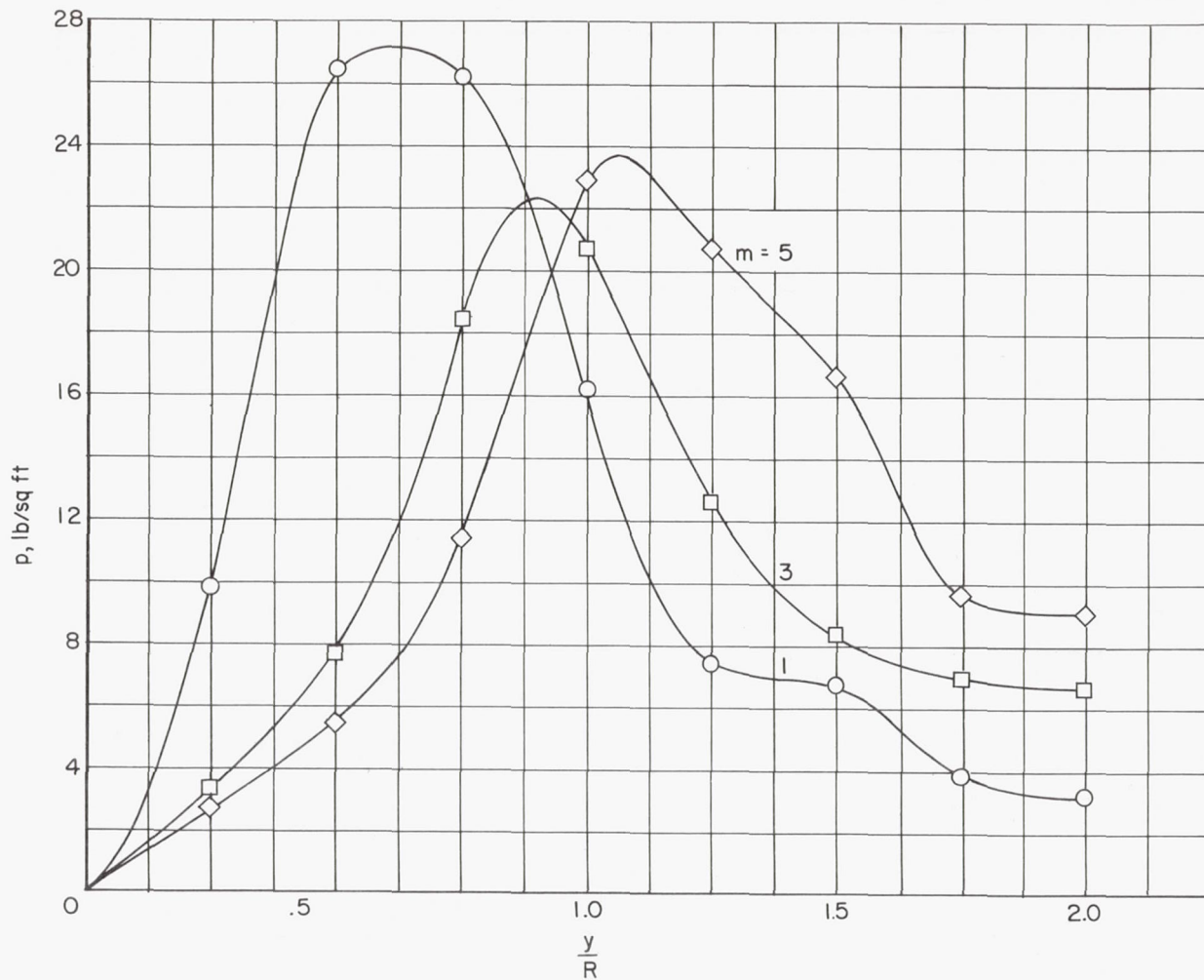


Figure 7.- Free-space root-mean-square oscillating pressure amplitude as a function of radial distance for three harmonics of a two-blade propeller. $x/R = 0.25$; $D = 3.5$ ft; $M_t = 1.10$; $C_p = 0.056$.

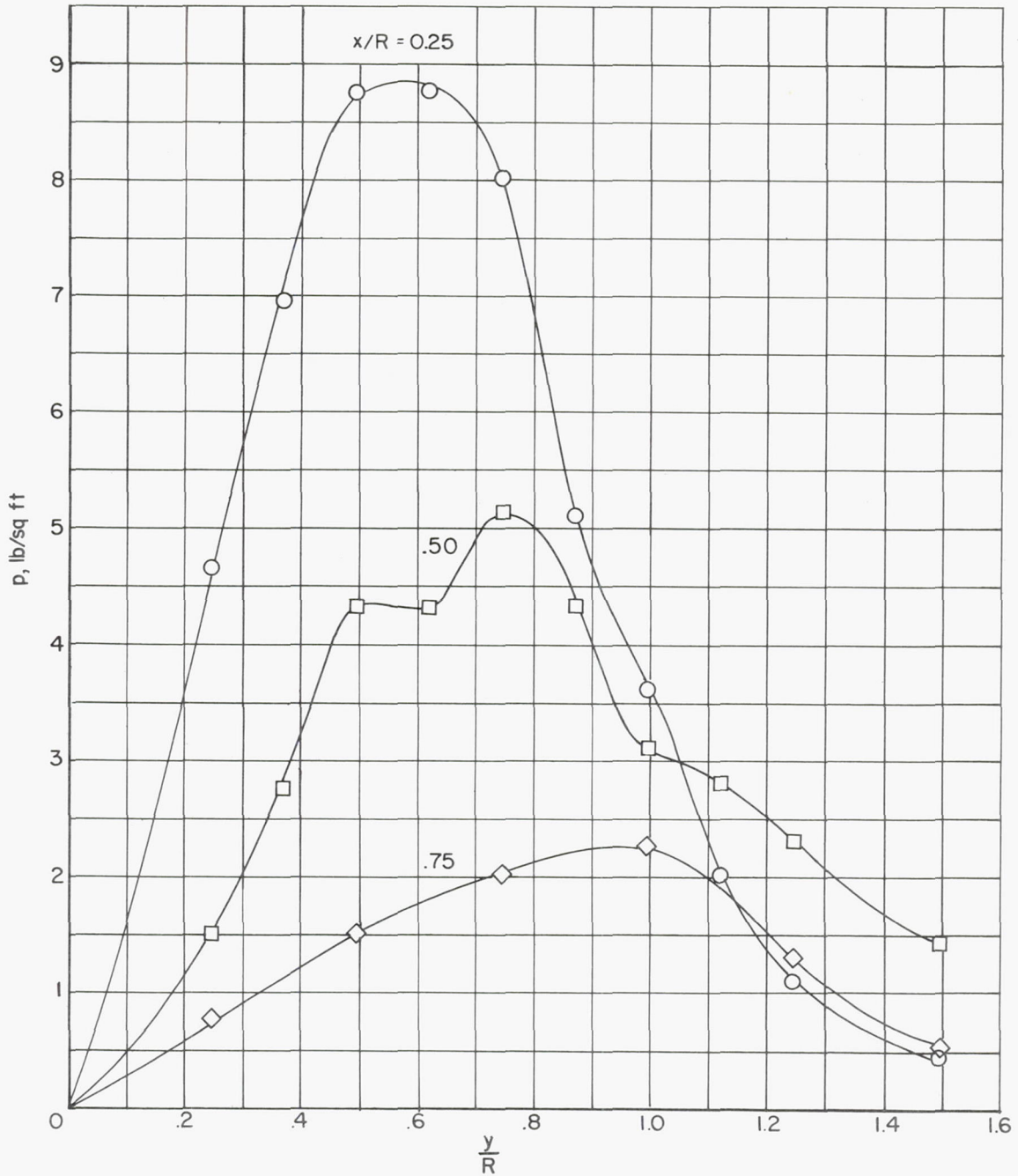
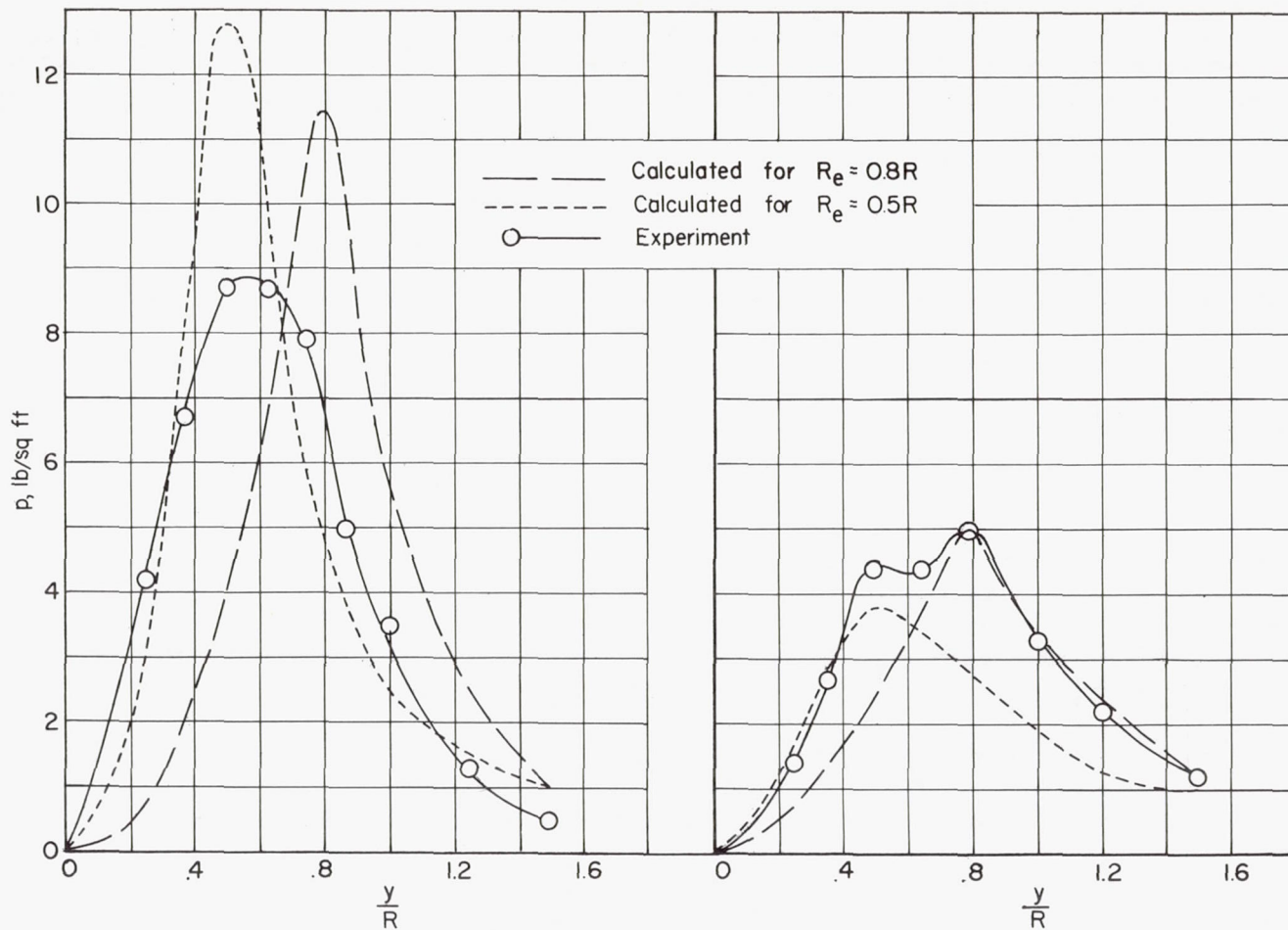


Figure 8.- Free-space root-mean-square oscillating pressure amplitude as a function of radial distance for three different axial stations.
 $D = 3.92$ ft; $M_t = 0.90$; $C_p = 0.058$; $m = 1$.



(a) $x/R = 0.25$.

(b) $x/R = 0.50$.

Figure 9.- Comparison of calculated and measured distributions of free-space root-mean-square oscillating pressures for the fundamental frequency of a two-blade propeller at two values of axial distance for a tip Mach number of 0.90. $D = 3.92$ ft; $C_p = 0.058$.

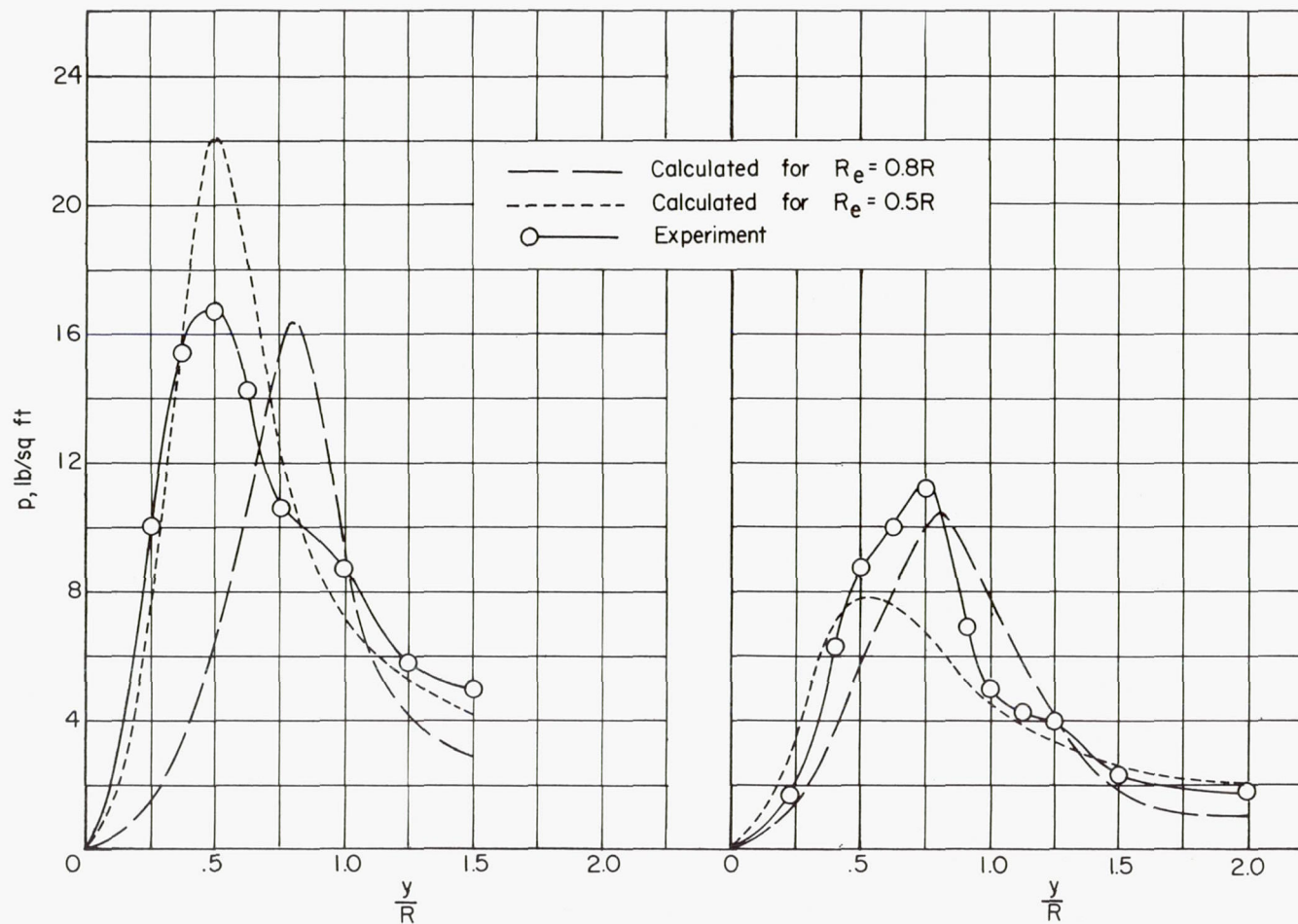
(a) $x/R = 0.25$.(b) $x/R = 0.50$.

Figure 10.- Comparison of calculated and measured distributions of free-space root-mean-square oscillating pressures for the fundamental frequency of a two-blade propeller at two values of axial distance for a tip Mach number of 1.20. $D = 3.92$ ft; $C_p = 0.069$.

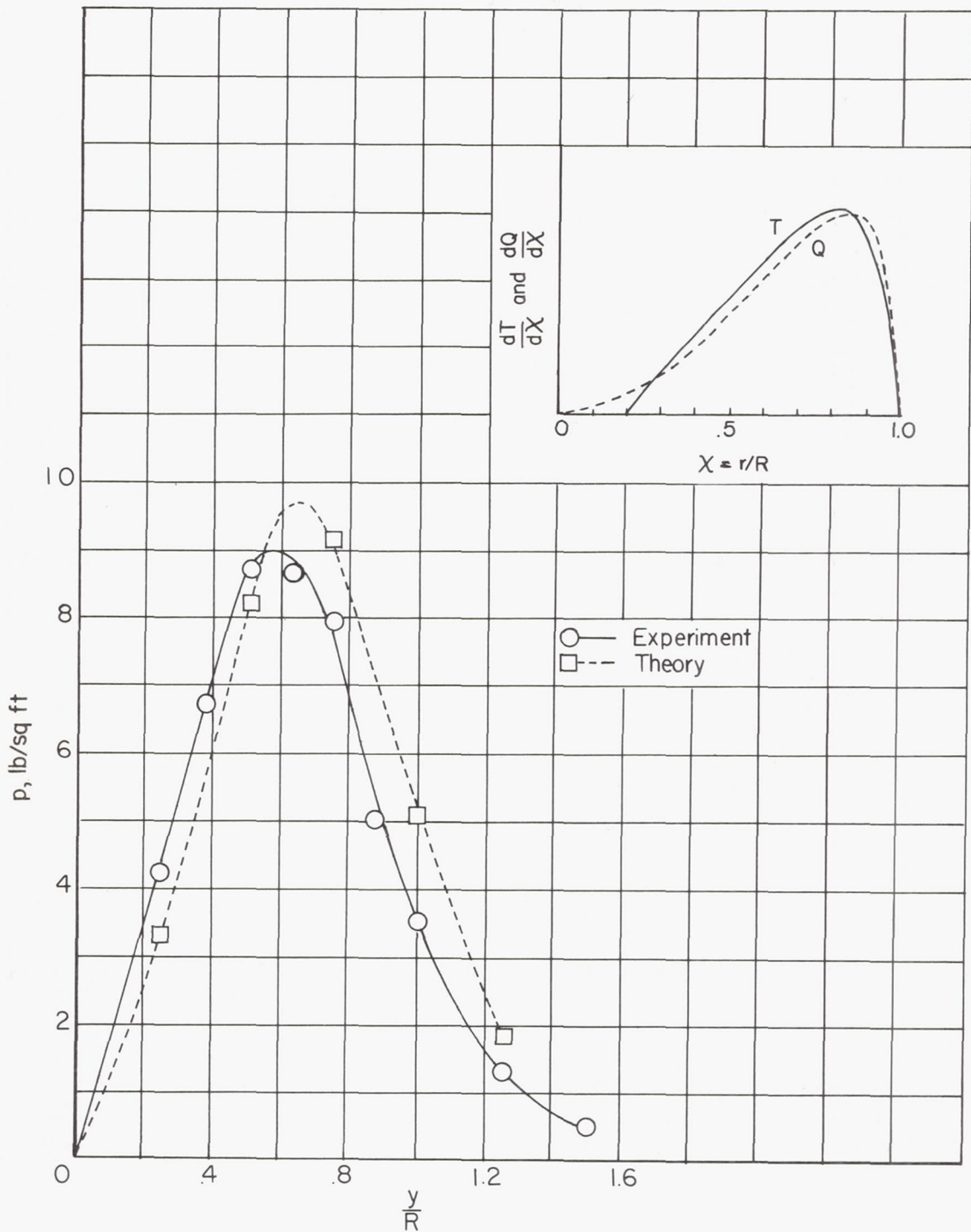


Figure 11.- Measured free-space root-mean-square oscillating pressure amplitudes of the fundamental frequency of a two-blade propeller as a function of radial distance compared with calculations based on a given torque and thrust distribution. $D = 3.92$ ft; $M_t = 0.90$; $x/R = 0.25$; $C_p = 0.058$.

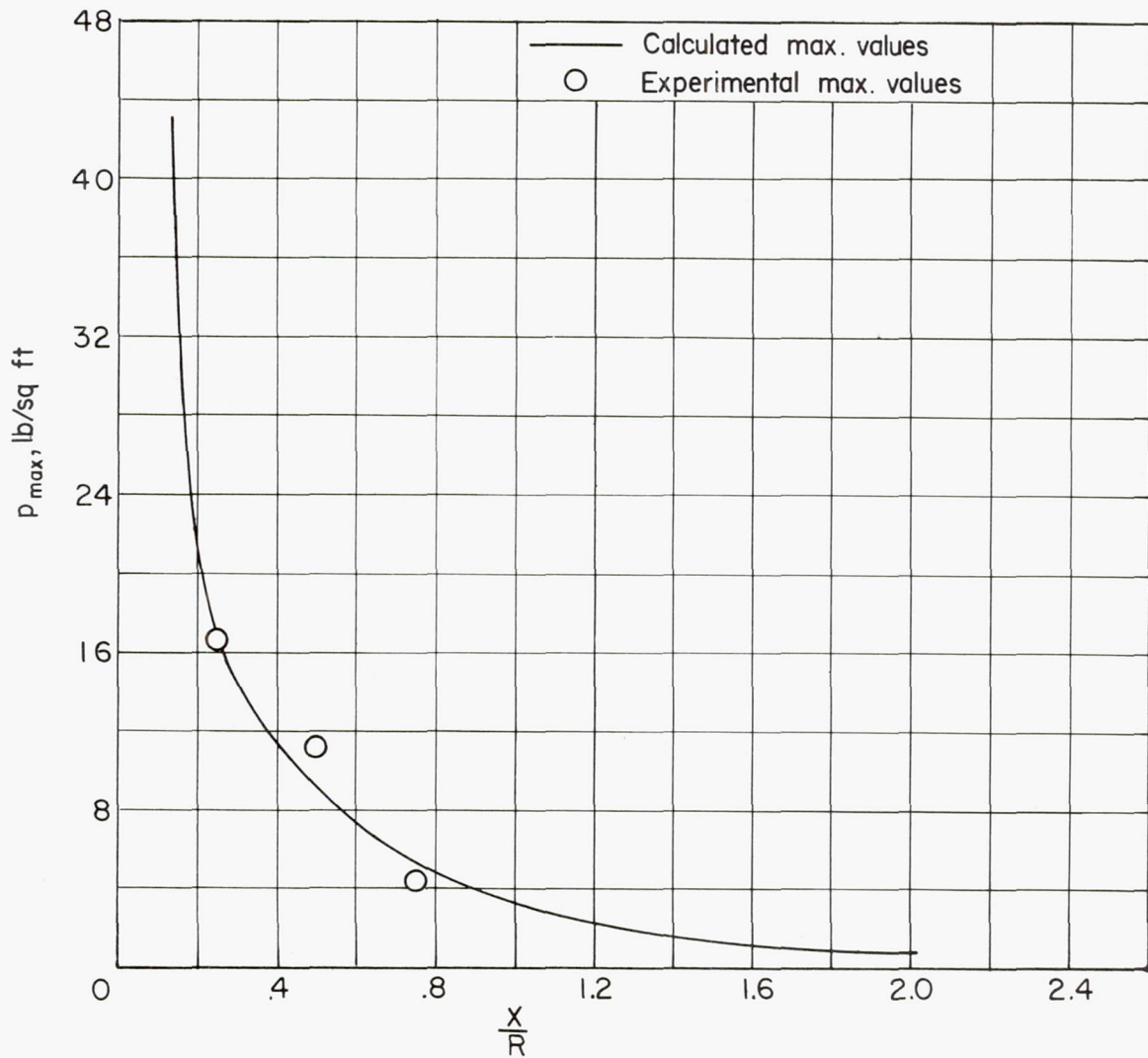


Figure 12.- Maximum free-space root-mean-square pressure amplitude of the fundamental frequency of a two-blade propeller as a function of axial distance from the propeller. $M_t = 1.20$; $D = 3.92$ ft; $C_p = 0.069$.

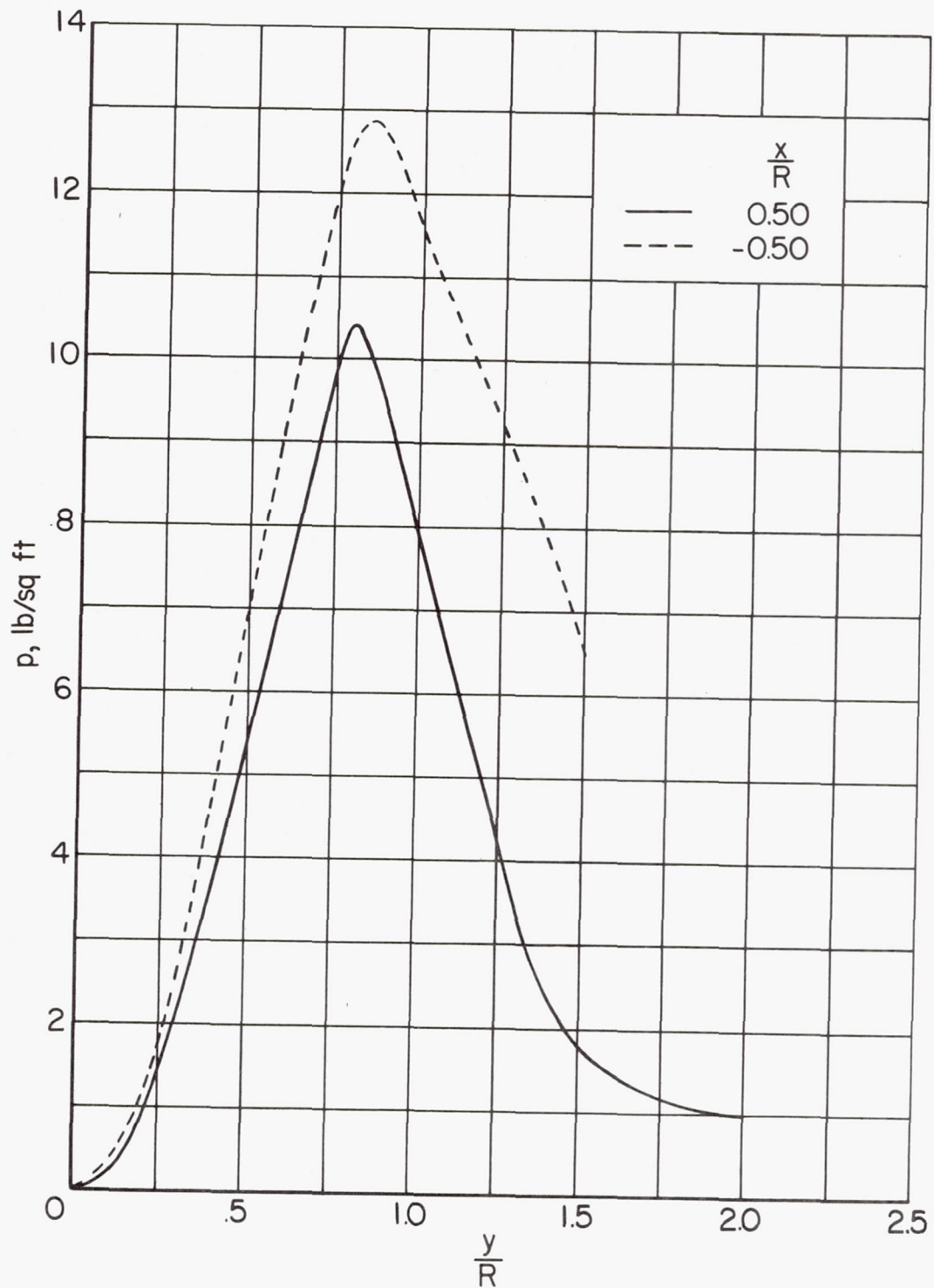


Figure 13.- Comparison of calculated free-space root-mean-square oscillating pressure magnitudes for the fundamental frequency of a two-blade propeller at equal axial distances ahead of and behind the propeller. $M_t = 1.20$; $D = 3.92$ ft; $C_p = 0.069$.

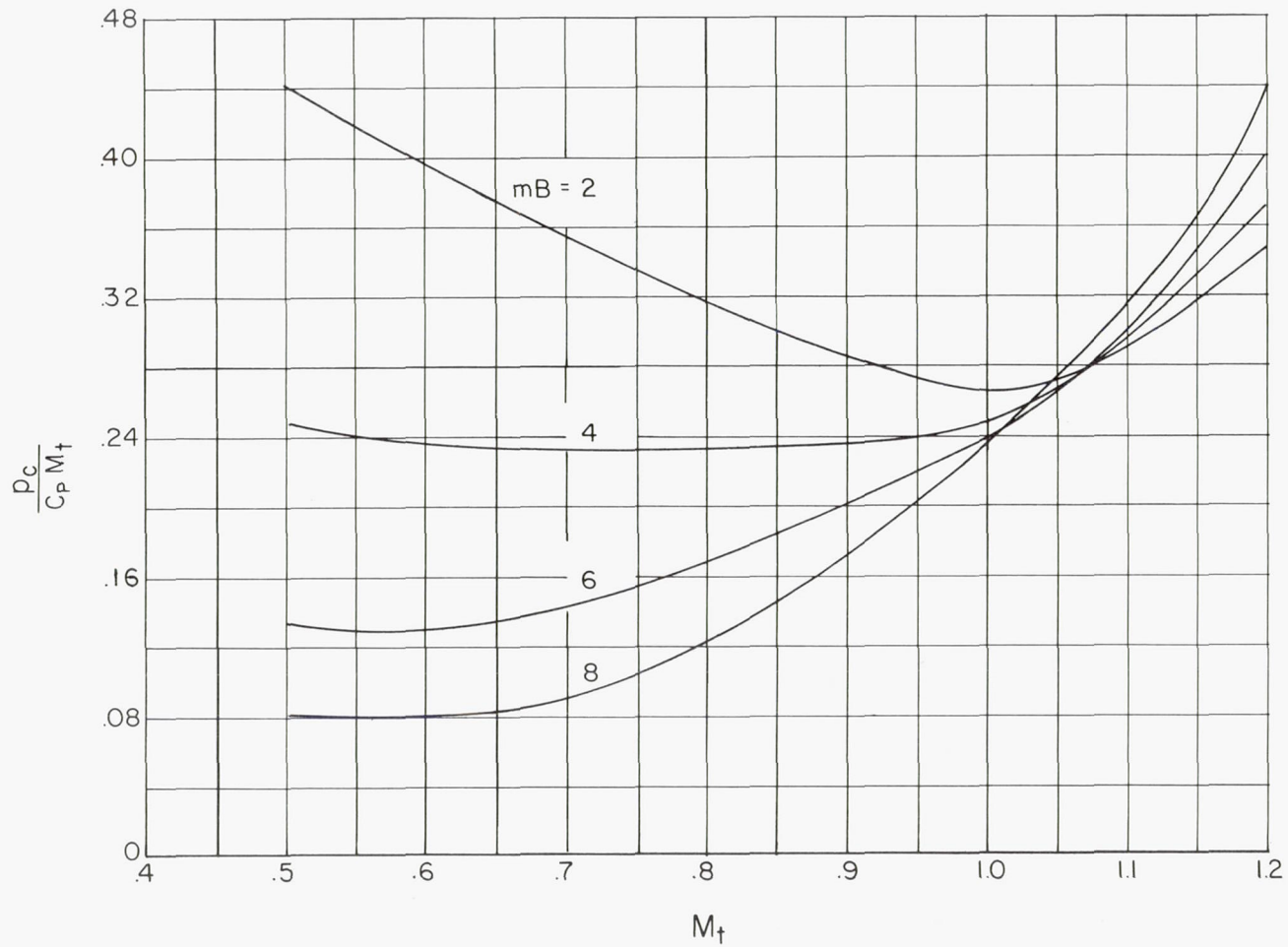


Figure 14.- Effect of tip Mach number at constant power on the free-space root-mean-square pressure amplitudes of the fundamental frequencies of propellers with various numbers of blades in the region where a fuselage might be located. $d/D = 0.10$.

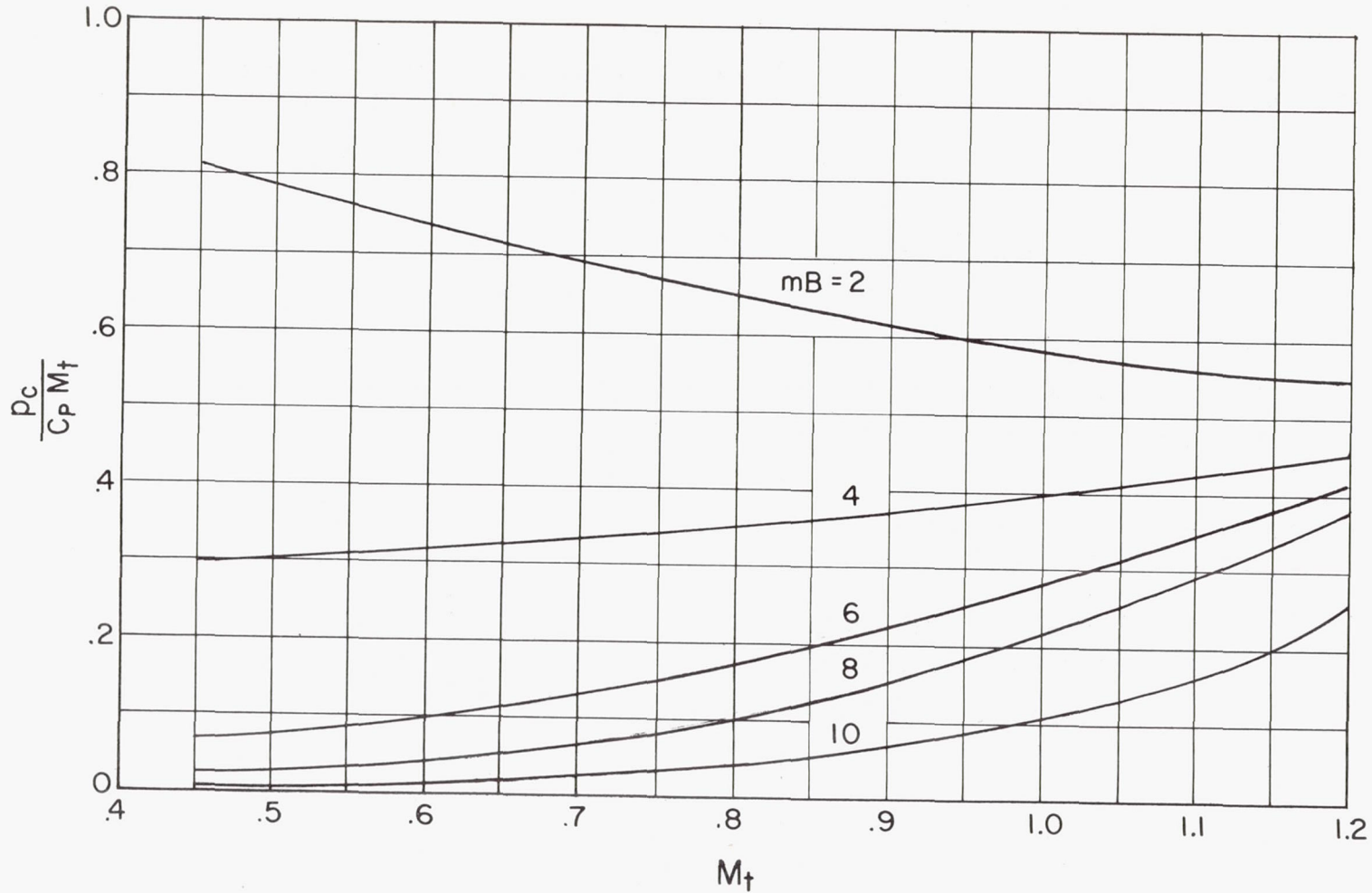
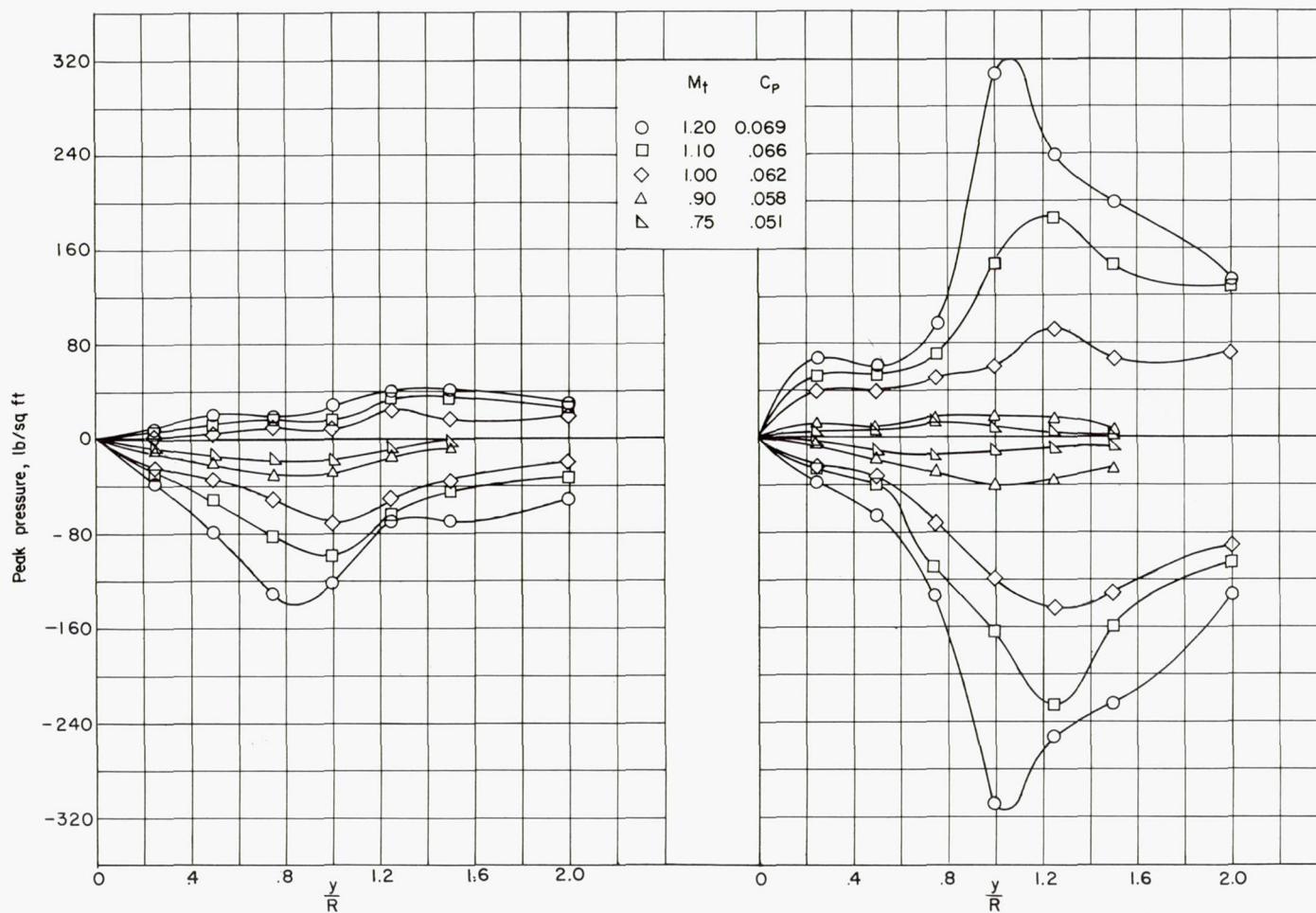


Figure 15.- Effect of tip Mach number at constant power on the maximum free-space root-mean-square pressure amplitude of the fundamental frequencies of propellers with various numbers of blades in the region where a wing might be located. $x/R = 0.50$.



(a) Surface from which blade recedes.

(b) Surface approached by blade.

Figure 16.- Distribution of peak values of oscillating pressure at the surfaces of a thin wing due to a propeller blade passage, for several values of propeller tip Mach number. $D = 3.92$ ft.

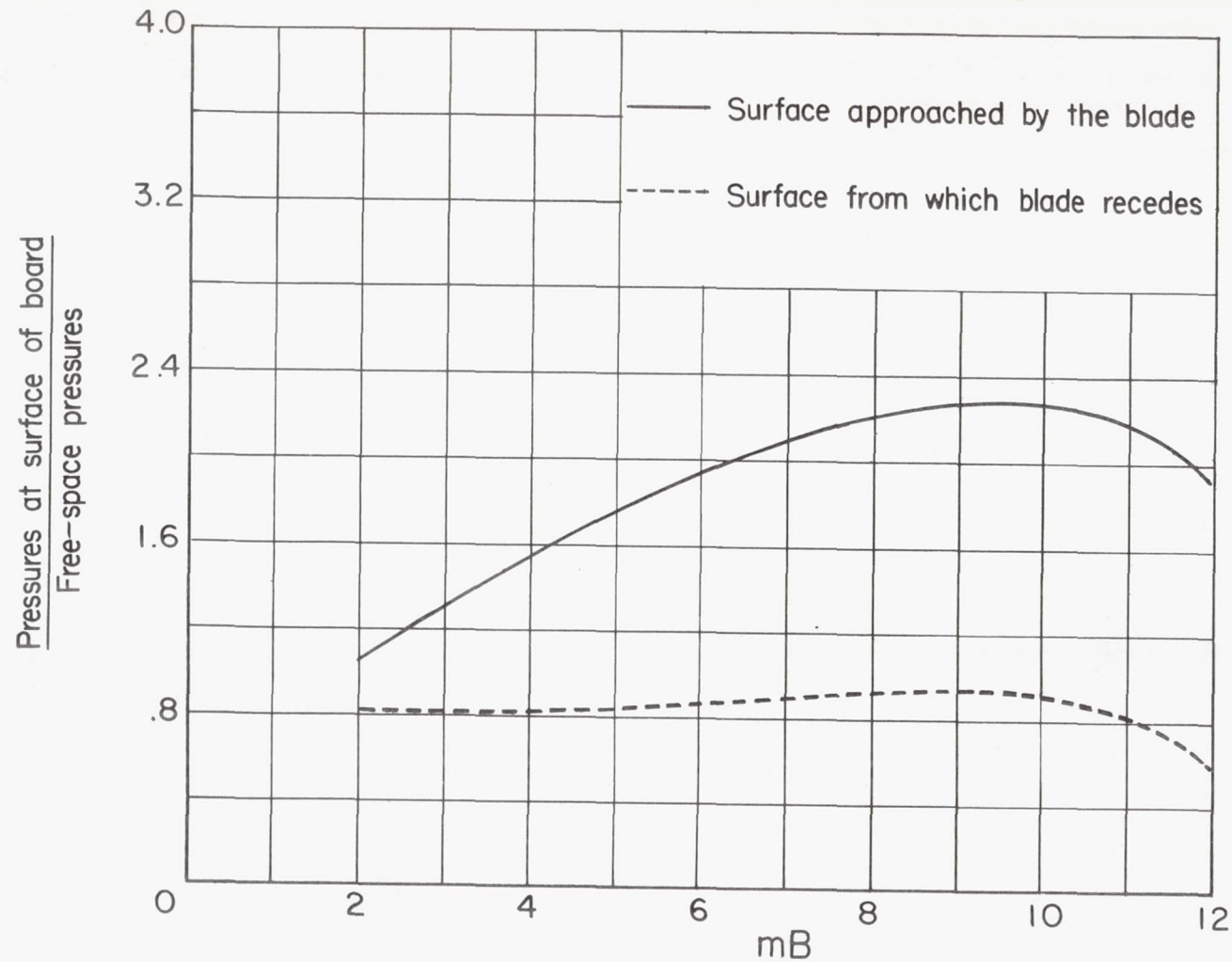


Figure 17.- Ratios of the root-mean-square oscillating pressure amplitudes at the surfaces of a thin wing to the corresponding free-space values for various harmonics of a two-blade propeller.

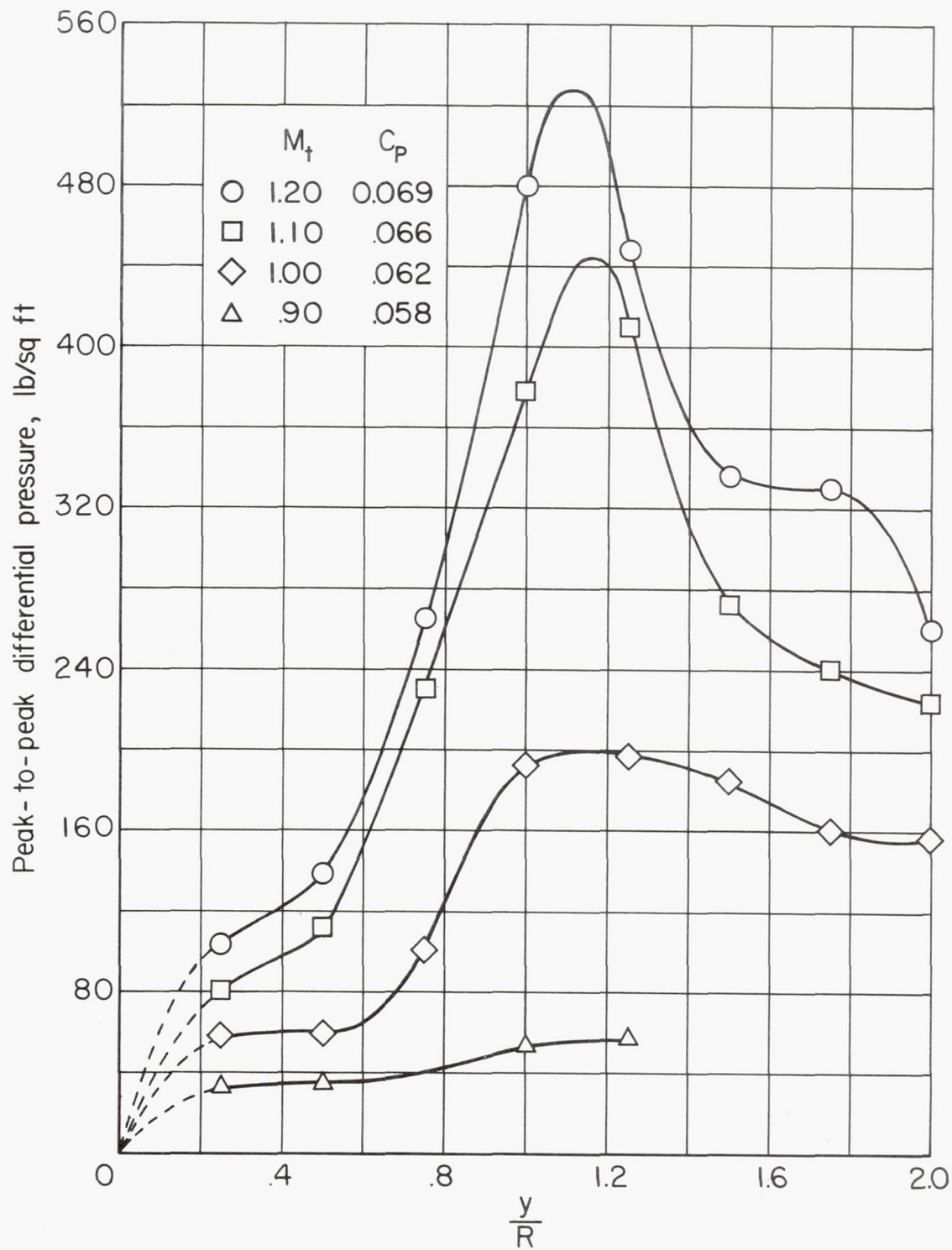
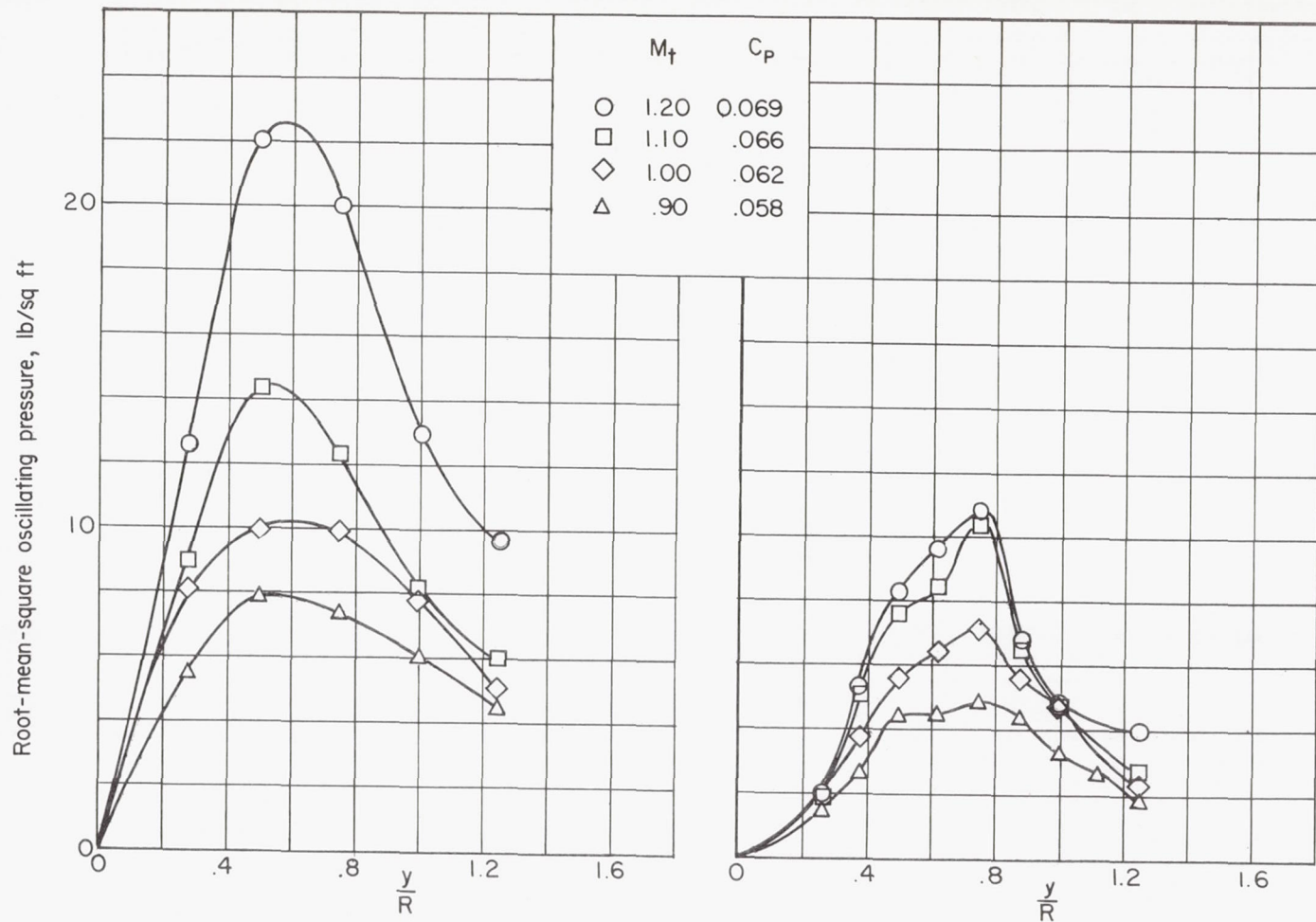


Figure 18.- Peak-to-peak differential pressures for a two-blade propeller measured across a thin wing as a function of radial distance for various tip Mach numbers. $x/R = 0.50$; $D = 3.92$ ft.



(a) Differential pressures.

(b) Free-space pressures.

Figure 19.- Comparison of the differential root-mean-square pressures across a thin wing with the free-space values at the same field points for the fundamental frequency of a two-blade propeller. $D = 3.92$ ft; $x/R = 0.50$.